2026 IEEE/SICE International Symposium on System Integration (SII)
January 11-14, 2026. Cancún, México

Textile-Based Strain Sensor for Real-Time Bending Angle Monitoring of Soft Joints

Claudia Sánchez[1], Jaime González[1], Jorge Muñoz[1], Santiago Martínez[1] and Concepción A. Monje[1]

Abstract— **This paper presents the design, fabrication, and evaluation of a textile-based strain sensor integrated into a soft robotic joint for real-time monitoring of bending angles. The proposed sensor consists of a conductive fabric encapsulated in a flexible silicone substrate, created using a custom co-casting process that enables seamless integration without compromising structural compliance. Electromechanical characterization under tensile and compressive loading demonstrated a strong piezoresistive response, with a gauge factor (GF) of 77.76 under tensile strain and 9.24 under compression, within working ranges of 6–12% and 3–14%, respectively. The sensor was embedded into a soft joint with asymmetric geometry to assess directional sensitivity and real-time performance. Experimental results confirmed reliable bidirectional strain detection and an over 500% increase in resistance under tensile bending. A second-order polynomial model accurately mapped the sensor's resistance changes to joint bending angles (10°–25°), achieving R^2 values above 0.67 in both tensile and compressive configurations. These findings validate the sensor's potential for real-time posture estimation in wearable and soft robotic systems.**

I. INTRODUCTION

Soft robotics is an innovative field of research that offers creative solutions to traditional robotic applications such as manipulation or wearable devices with the use of soft structures. Even though traditional rigid-link manipulators excel at positioning accuracy, soft-link actuators can adopt a variety of shapes, adapt to complex structures, absorb a greater amount of impact without compromising structural integrity, and safely interact with biological tissues, all while still offering precise positioning [1].

Due to the complexity of soft-robotic actuators, there is interest in monitoring the deformation of the structure[2]. This necessity translates into the introduction of different embedded sensors inside the soft structures. However, introducing rigid sensing elements limits the original cinematic behaviour of the soft actuator, negating their advantages over traditional ones. Commercial strain gauges need mounting housings or rigid backings that limit local compliance and impair the actuator's ability to conform to complex surfaces or absorb unintended impacts, since these could compromise the sensor. These problems motivate the development of sensing solutions that are intrinsically soft, as well as seamlessly integrated within the actuator's body.

The field of soft sensors focuses on "sensing through structure," where deformable materials themselves act as the transduction medium. One approach is to use embedded conductive channels within soft silicone matrices to create sensors whose electrical properties change with bending and stretching, eliminating rigid interfaces and preserving overall compliance [3]. Reviews of flexible pressure and strain sensors highlight similar approaches, emphasizing that in situ integration not only protects the sensing element from environmental damage but also distributes mechanical stress uniformly, thereby improving durability under cyclic loading [4]. Nevertheless, generating a reliable, low-hysteresis sensing over large strains remains challenging, especially when balancing sensitivity, response speed, and mechanical robustness in one single soft package [5]. One line of soft-sensor research is the use of conductive fabric materials, which can be integrated inside plastic materials due to their flexible nature. Resistive textile sensors transduce deformation into a measurable change in electrical resistance, offering simple readout electronics and straightforward process of fabrication on flexible substrates. Such sensors have already been developed and integrated into soft-link actuators, proving that bending-induced elongation of the elastomer produced a monotonic increase in resistance, which enabled finger-angle estimation and demonstrated robustness over hundreds of cycles [6], [7]. Some lines of research include coating methods to provide textile fibers with conductive properties, using metal nanoparticle inks, conductive polymers or carbon-based materials. Other studies suggested the combination of conductive, metallic fibers into stretchable fabrics, pointing toward integrated solutions for wearable textile-based soft sensors and actuators [8], [9], [10].

Sensor encapsulation protects the sensing element from environmental factors and distributes mechanical loads, preventing localized failure. Some common encapsulation techniques are lamination, where a thin elastomeric film is bonded over the sensor; overmolding, in which liquid silicone is cast directly on the sensor; and co-casting, which embeds the sensor within the actuator material during fabrication. Co-casting can achieve seamless monolithic structures but requires precise control over curing conditions to avoid voids or misalignment [11]. Overly stiff overmolds can introduce stress concentrations at the sensor–actuator interface, leading to signal artifacts or premature delamination. Conversely, insufficient encapsulation leaves conductive traces exposed, increasing the risk of mechanical damage or electrical shorting under cyclic deformation [12].

Despite significant progress in soft-sensor materials and fabrication, there remains a lack of textile-based strain sensors that are encapsulated within soft actuators without sacrificing function or durability. In addition to this, commercial alternatives are often expensive and limited to

[1]These authors are with the Department of Systems Engineering and Automation, RoboticsLab, Carlos III University of Madrid, Av. de la Universidad, 30, 28911 Leganés, Madrid, Spain. clausanc@ing.uc3m.es

certain morphologies. In this work, this gap is addressed with a new textile-based sensor integrated inside a cylindrical silicone sleeve through a co-casting process. The proposed sensor benefits from the flexibility and conductiveness of a metallic fabric with the protection of a soft polymeric material that does not limit the movement of the fabric. When integrated into a cable-driven soft joint, the sensor provides measurable flexion–extension feedback with high tensile sensitivity, while exhibiting the typical hysteresis and nonlinearities of elastomer-based piezoresistive materials.

II. MATERIALS AND METHODS

A. Materials

The textile sensor consists of a non-woven polyamide fabric that is coated and bonded with copper and nickle, making it electrically conductive while retaining the flexibility of regular fabric. These properties make this material interesting for the development of flexible sensors. The material, called Shieldex® Nice, is distributed by the company Shieldex® [13], and the technical specifications of this material are included in Table I.

TABLE I

SHIELDEX®NICE PROPERTIES.

Property	Value
Material Composition	(55% PA / 44% Cu / + 1% Ni) ± 15%
Electrical Surface Resistivity	$< 0.02\ \Omega/m^2$
Temperature Range	−30 °C / 90 °C
Total Weight	$105\ g/m^2 \pm 20\ \%$
Total Thickness	0.35 mm ± 20 %

In this work, this textile sensor is encapsulated in a silicone substrate that protects it and provides it with structure, allowing it to be integrated into soft bodies without compromising the integrity of the textile sensor inside it. The silicon substrate is made of Ecoflex™ Fast 00-35 Gel, comercialized by Smooth-on® [14], and the parameters of interest of this material are included in Table II.

TABLE II

TECHNICAL OVERVIEW OF THE ECOFLEX™ FAST 00-35 GEL.

Property	Value
Mixed Viscosity	3.5 Pa·s
Specific Gravity	$1070\ kg/m^3$
Specific Volume	$9.39 \times 10^{-4}\ m^3/kg$
Shore Hardness	00-35 (dimensionless)
Tensile Strength	1.38 MPa

B. Fabrication of the Textile-based Sensor

To fabricate the sensor, a mold was designed using Autodesk Fusion 360, consisting of a two-piece enclosure with a hollow cylindrical shape contained in between the two parts. The cylinder had a diameter of 5.8 mm and length of 70 mm, to match the size of the textile part of the sensor. The mold was 3D printed using polylactic acid (PLA).

The first component in the making of the flexible sensor is the textile portion. For the sensor, the flexible fabric is cut into 55x5.8 mm rectangular strips. These strips will be soldered to cables for the measurement of the electrical resistivity of the sensor. The second component is the silicon mixture. The composition of the substrate consists on a mixture of two gel ingredients which once combined cure at room temperature, solidifying into a plastic product. This happens in a small time window, with the mixture having a liquid-state life of 2.5 minutes and a cure time of 5 minutes.

The fabrication process of the textile-based sensor is illustrated in Fig. 1. It starts with the mixture of the silicone substrate, following the 1:1 ratio established by the manufacturer. Once the two parts of the material are combined, the mixture is poured into the lower half of the two-piece PLA cylindrical mold, filling the longitudinal half-cylinder cavity. Before the material hardens, the strip of conductive fabric is laid on top of the surface of the silicone substrate, while keeping the pre-soldered ends and cables outside of the mold. Due to its viscous state, the silicone substrate allows for the slight submersion of the fabric by applying a small amount of pressure, causing the strip to become embedded to the silicone with a slight displacement from the central axis of the mold. Following the placement of the sensor into the mold, the remaining substrate is poured into the top half of the mold. The molds are then aligned and clamped together, completing the cylindrical shape while the material is still in a soft state, allowing the uncured silicone from both sides to merge and form a continuous cylinder. The molds are fastened together to ensure geometrical regularity.

After curing, the cylindrical sensor is removed and any excess material is trimmed as needed. This concludes the fabrication process of the sensor.

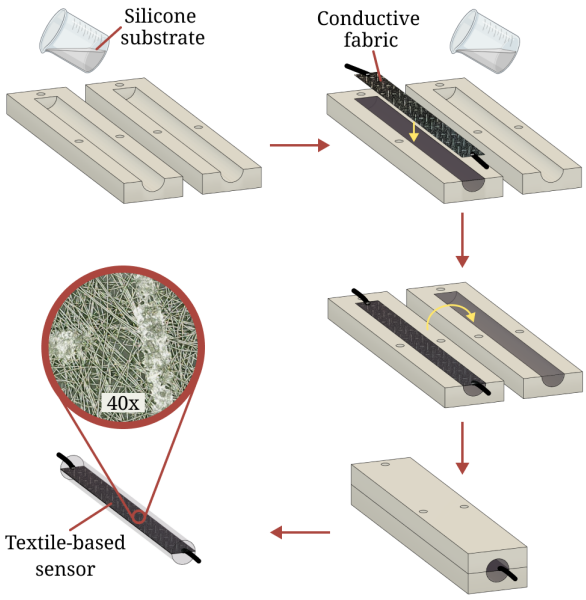

Fig. 1. Schematic of the fabrication of the textile sensor, showing the steps of the process to obtain the final product.

C. Electromechanical Testing

The electromechanical characterization was conducted by measuring the variation in electrical resistance of the textile-based strain sensor under controlled uniaxial tensile and compressive loading at ambient temperature. Samples were tested using a Universal Testing Machine (Instron Model 34SC-1, Norwood, USA) equipped with a 1 kN load cell at a constant strain rate of 100 mm/min. Electrical resistance data were collected simultaneously using an in-situ data logger (DataTaker DT82 Series 4, Thermo Fisher Scientific, Australia), configured in a four-probe arrangement, which effectively eliminated the influence of lead wire resistance. Integration of the resistance measurements with the mechanical testing machine was achieved via a BNC connection, enabling synchronized acquisition of both resistance and displacement data at a sampling frequency of 5 Hz. Experiments for monitoring the bending angle of the soft joint using the textile-based flex sensor were conducted on the Universal Testing Machine (UTM). A custom-designed fixture, integrated with standard three-point bending test attachments, was employed to induce controlled bending and enable accurate tracking of the resulting angular displacement.

III. RESULTS AND DISCUSSION

A. Textile-Based Sensor Characterization

The directional bending response of the textile-based strain sensor was evaluated using the setup illustrated in Fig. 2. To assess the response under different strain modes, the sensor, composed of a cylindrical silicone substrate with a conductive fabric film embedded, was manually repositioned so that the conductive fabric faced either the outer (convex) or inner (concave) side of the bending arc. When positioned on the convex side, the conductive fabric underwent tensile strain as it stretched during bending. In contrast, when positioned on the concave side, it experienced compressive strain as it was compressed. In both cases, bending was induced by the vertical displacement of the upper clamp in the Universal Testing Machine (UTM), which altered the curvature and chord length of the sample. This configuration enabled controlled evaluation of the sensor's electromechanical response to directional bending (see Fig. 3a).

The strain (ε) experienced by the sensing layer during bending was computed based on its geometric position relative to the neutral axis, as given in (1).

$$\varepsilon = \pm \frac{h}{r} \tag{1}$$

where h is the distance from the neutral axis to the sensing layer, and r is the radius of the curvature of the bent structure [15], [16]. The curvature radius r was derived from the geometric relation shown in (2), which relates the measured chord length c and arc length L of the bent sensor.

$$c = 2r \sin\left(\frac{L}{2r}\right) \tag{2}$$

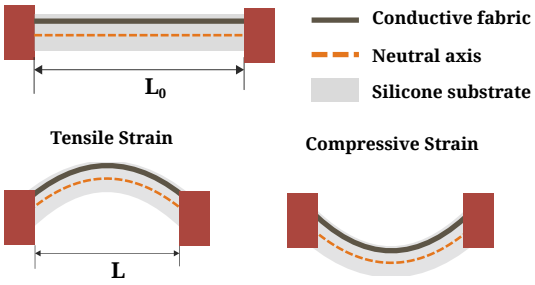

Fig. 2. Schematic of the textile-based sensor under bending. The sensor's performance depends on the deformation experienced by the conductive fabric layer, which undergoes tensile strain when oriented on the convex side and compressive strain when on the concave side relative to the neutral axis.

In this work, the fabricated sensor has an arc length of 55 mm, and the h value is assumed to be 2 mm. During testing, the cord length was reduced from 55 mm to 25 mm in both directions. As illustrated in Fig. 3b, the sensor demonstrates a clear piezoresistive response to bending deformation: the electrical resistance increases during outward bending and decreases during inward bending.

To quantify the strain sensitivity of the textile-based sensor, the gauge factor (GF) was calculated as defined in (3).

$$GF = \frac{\Delta R/R_0}{\varepsilon} \tag{3}$$

where ΔR is the change in resistance, R_0 is the initial resistance, and ε is the applied strain. Because the sensor response is nonlinear, the $\Delta R/R_0 - \epsilon$ curve was divided into linear segments, and the GF in each segment was obtained as the slope of the corresponding linear fit (Fig. 3c-d). Under tensile loading, the sensor showed a high GF of 77.76 (Fig. 3c), with a linear response, indicating strong sensitivity to elongation within a working range of 6% to 14% strain. In contrast, during compressive deformation, the sensor exhibited a lower GF of 9.24, but over a broader working range of 3% to 14%, as shown in Fig. 3d. This asymmetric behavior can be attributed to the microstructural and conductive properties of the Shieldex® Nice fabric. Under tensile strain, the fabric structure stretches, and micro-cracks form in the metal coating, disrupting the conductive pathways and leading to a sharp increase in resistance. Additionally, the random orientation of the fibers further amplifies this effect by causing localized strain concentration and fragmentation of the conductive network. Conversely, under compressive strain, the fibers tend to buckle or fold; however, the resulting increase in contact area is less consistent and spatially nonuniform, resulting in a more moderate and less linear decrease in resistance. To evaluate the repeatability of the sensor under compressive deformation, cyclic bending tests were performed at displacement amplitudes of 10 mm, 20 mm, and 30 mm. As shown in Fig. 3e, the sensor exhibited a repeatable decrease in relative resistance with increasing displacement. However, slight signal drift was observed across cycles, which may be attributed to mechanical stress at the soldering points and micro-movements of the

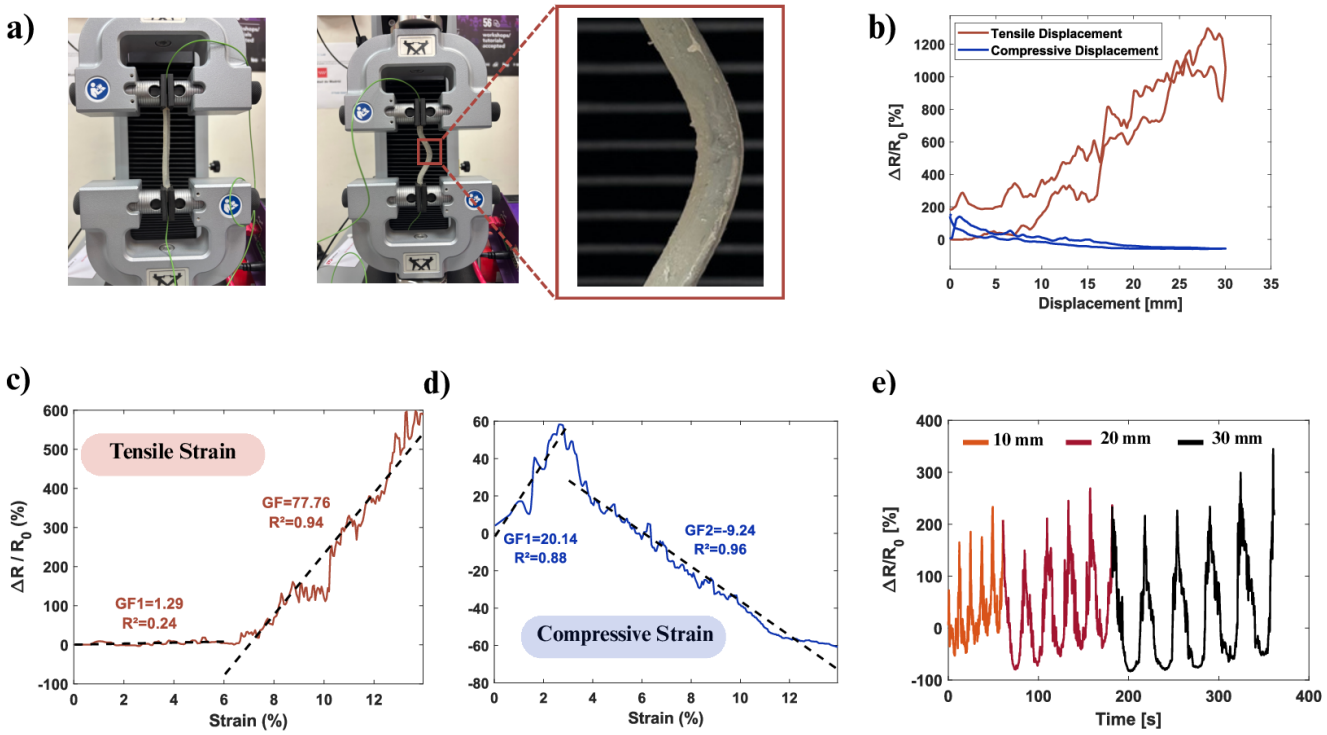

Fig. 3. Performance and sensing-strain properties of the textile-based strain sensor. (a) Test setup showing outward bending of the sensor under tensile loading. (b) Relative resistance variation of the textile-based sensor under compressive and tensile displacement (c-d). Sensitivity of the textile-based sensor and its multi-segment linear fitting curves. GF and fitting degree (R^2) are included. (e) Relative resistance changes under various cyclical displacements (10mm - 20mm - 30 mm) for the textile-based strain sensor.

wire connections, issues commonly encountered in flexible sensing systems.

B. Bending Angle Estimation

The textile-based sensor's capability for real-time posture estimation was evaluated through integration into a soft joint developed at the RoboticsLab of the Carlos III University of Madrid [17], [18]. This soft joint features an asymmetrical prismatic morphology composed of a series of triangular-section links connected by a compliant central axis. The design supports multi-directional bending with two degrees of freedom (DOF), actuated by tendons routed through the asymmetric sections. This geometry not only enables complex motion but also provides inherent mechanical protection against extreme loads.

For testing, the soft joint was fabricated with an internal channel to allow manual insertion of the textile-based sensor along the central curvature path. This integration ensured that the sensor remained fixed in a known position and was aligned with the principal bending axis. To replicate tendon-driven bending, a custom experimental setup was developed using a 3D-printed fixed frame with a rotating base (Fig. 4), integrated into the UTM. One end of the soft joint was fixed to the rotating base, while the UTM vertically compressed the other to induce bending. The rotating base enabled testing of two distinct configurations without altering the sensor's initial location (see Fig. 5a):

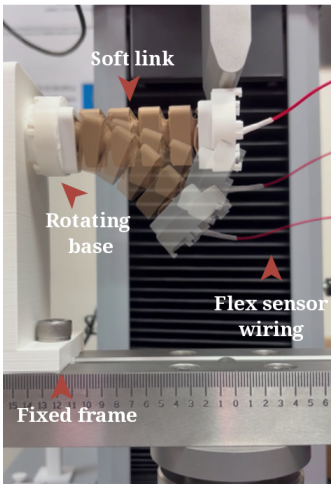

Fig. 4. Setup for bending angle estimation of the soft joint. The joint, composed of soft links, is mounted on a rotating base fixed to a support frame, while the textile-based sensor is embedded along the curvature. The conductive fabric is oriented to face the edges of the soft link to ensure directional strain response during bending.

- **Configuration A**: The joint was oriented so that the load was applied to the edges, causing it to bend toward the vertices of the triangular cross-sections. In this configuration, the conductive fabric faced the convex side of the bend and experienced tensile strain, resulting

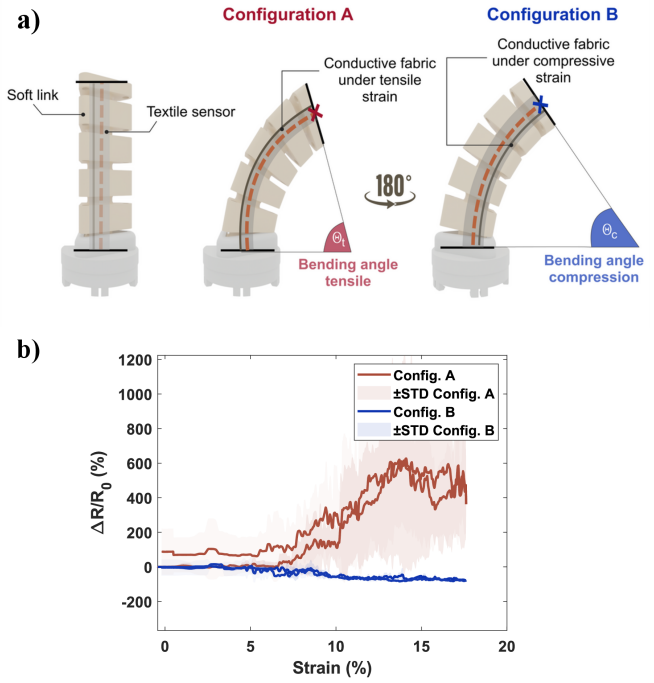

Fig. 5. a) Schematic of the two tested configurations: Configuration A applies force to the edges, bending the joint toward the vertices and placing the conductive fabric under tensile strain. Configuration B rotates the joint 180°, applying force to the vertices and bending toward the edges, placing the conductive fabric under compressive strain. The bending angle (θ) is defined as the angle between the base and the tip of the joint for tensile (θ_t) and compressive (θ_c) deformation of the sensor. b) Relative resistance response of the sensor for each configuration. Solid lines represent mean values; shaded regions indicate standard deviation across trials.

in an expected increase in resistance.

- **Configuration B**: The joint was rotated 180°, and the load was applied to the vertices, causing it to bend toward the edges. In this case, the conductive fabric faced the concave side of the bend and experienced compressive strain, leading to a decrease in resistance.

The sensor's response under tensile and compressive strain is shown in Fig. 5b, corresponding to configurations A and B, respectively. In the tensile case, the relative resistance increased by over 500% up to 14% strain, matching the working range limit established during the uniaxial tests. This amplified response suggests that embedding the sensor within the joint improves strain transfer and enhances piezoresistive sensitivity due to guided and localized deformation. However, the response exhibited high variability across three repetitions, indicating poor repeatability under tensile loading, likely due to localized strain and structural instability. In contrast, compressive bending resulted in a more stable and consistent decrease in resistance of approximately 80%, aligning with the sensor's previously observed behavior under compressive strain. These results confirm the sensor's ability to detect bidirectional bending, highlighting its sensitivity despite limitations in repeatability.

Building on this directional strain response, the textile-based sensor's ability to track joint posture was evaluated by correlating its resistance resistance with the joint's bending

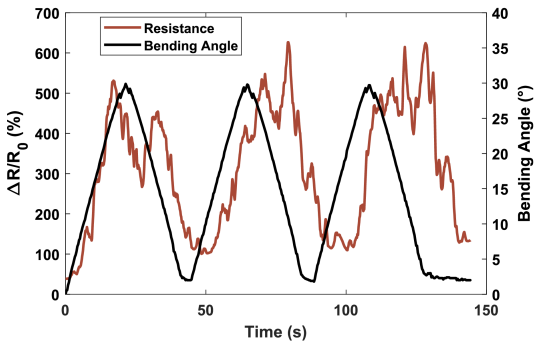

Fig. 6. Real-time correlation between sensor resistance and bending angle over multiple actuation cycles for Configuration A.

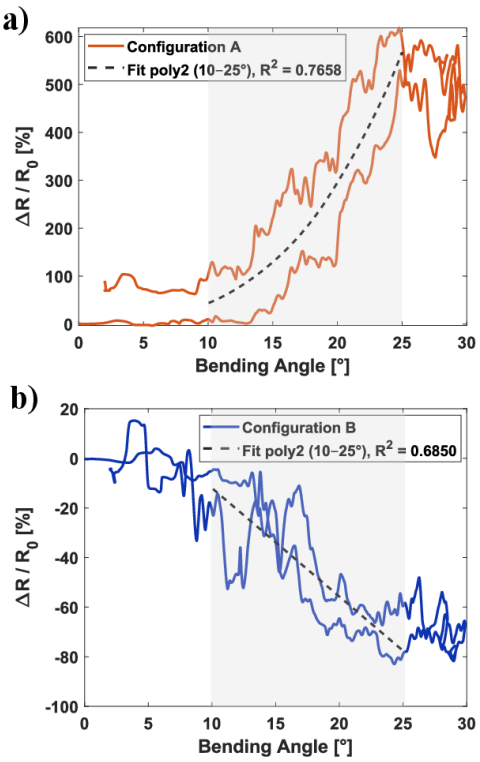

Fig. 7. Fitted polynomial models for bending angle estimation from relative resistance data for a) textile-based sensor tensile strain and b) textile-based sensor compressive strain. The gray shaded region denotes the 10°–25° working range

angle. Fig. 5a illustrates the method used to estimate the bending angle (θ), defined as the angle formed between the neutral axis at the base of the link and the position of the tip in the bent configuration. Real-time tracking was obtained from video analysis, and its correlation with the sensor's relative resistance is presented in Fig. 6. To model this relationship, second-order polynomial fits were applied to the average relative resistance data within the monotonic $10° - 25°$ working range. As shown in Fig. 7a-b, the fits showed good agreement in both configurations, with coefficients of determination (R^2) of 77% and 68% for configurations A and B, respectively. These results con-

firm a good, consistent, and direction-dependent correlation between angle and resistance, validating the sensor's use for continuous bending angle estimation in soft joints. The relative resistance-bending angle relationship was modeled using the quadratic equation given in (4).

$$\Delta R/R_0 = a\theta^2 + b\theta + c \tag{4}$$

were a, b, and c are the polynomial coefficients. The fitted parameters for both tensile and compressive cases are provided in Table III.

TABLE III

SECOND-ORDER POLYNOMIAL COEFFICIENTS FOR THE RELATIVE RESISTANCE–BENDING ANGLE MAPPING.

Strain	**a**	**b**	**c**	R^2
Tensile	1.82	-28.98	152.47	0.77
Compressive	-0.001	-4.28	30.77	0.68

The second-order polynomial model offers a computationally efficient and memory-light solution for embedded real-time systems. The fitted coefficients enable direct calibration of the sensor, allowing resistance data to be mapped to bending angle within the defined working range. This approach supports integration into closed-loop control schemes and real-time posture estimation in soft robotic joints and wearable systems.

IV. CONCLUSIONS

This work has addressed the design, fabrication, and evaluation of a textile-based strain sensor for monitoring bending in soft joints. The sensor was fabricated by embedding a commercial conductive fabric onto a cylindrical silicone substrate using a custom mold. The electromechanical characterization under uniaxial loading demonstrated that the sensor exhibits strong piezoresistive behavior, with a highly sensitive response under tensile strain (GF = 77.76) and a lower (GF = 9.24), but stable, response under compression, with similar working ranges and determinant coefficients over 90%. These characteristics were preserved when the sensor was embedded into the soft joint, where directional bending induced distinct tensile and compressive strain states depending on the joint configuration. Notably, the sensor achieved a relative resistance increase of over 500% under tensile bending, exceeding the standalone characterization results due to enhanced strain localization. However, this amplification came at the cost of higher signal variability, indicating a trade-off between sensitivity and repeatability. The relationship between the resistance and the bending angle achieved by the soft joint was modeled using second-order polynomials for a working range of 10° to 25°, demonstrating the capability of the fabricated sensor to provide real-time feedback.

Future work will focus on evaluating alternative attachment methods for reliably interfacing with the conductive fabric to measure resistance changes. Techniques such as conductive adhesives, crimp connectors, and snap fasteners will be explored as replacements for conventional soldering, with the aim of reducing contact noise and enhancing both signal stability and sensor repeatability.

ACKNOWLEDGMENT

The research leading to these results has been supported by the SIROCO project, with reference PID2023-147343OB-I00, funded by MICIU /AEI/10.13039/501100011033 and FEDER, UE, and the ADAPTA project, with reference PLEC2023-010218, funded by MCIN/AEI/10.13039/501100011033.

REFERENCES

[1] C. Relaño, J. Muñoz, C. A. Monje, S. Martínez, and D. González, "Modeling and Control of a Soft Robotic Arm Based on a Fractional Order Control Approach," *Fractal and Fractional*, vol. 7, no. 1, p. 8.

[2] C. Sánchez, D. Rodríguez, S. Otero, and C. A. Monje, "A Piezoresistive Printable Strain Sensor for Monitoring and Control of Soft Robotic Links," in *2025 IEEE International Conference on Robotics and Automation (ICRA)*, pp. 16556–16562.

[3] R. Slyper, I. Poupyrev, and J. Hodgins, "Sensing through structure: Designing soft silicone sensors," in *Proceedings of the Fifth International Conference on Tangible, Embedded, and Embodied Interaction*, TEI '11, pp. 213–220, Association for Computing Machinery.

[4] W. Chen and X. Yan, "Progress in achieving high-performance piezoresistive and capacitive flexible pressure sensors: A review," *Journal of Materials Science & Technology*, vol. 43, pp. 175–188.

[5] J. Qin, L.-J. Yin, Y.-N. Hao, S.-L. Zhong, D.-L. Zhang, K. Bi, Y.-X. Zhang, Y. Zhao, and Z.-M. Dang, "Flexible and Stretchable Capacitive Sensors with Different Microstructures," *Advanced Materials*, vol. 33, no. 34, p. 2008267.

[6] Z. Shen, J. Yi, X. Li, M. H. P. Lo, M. Z. Q. Chen, Y. Hu, and Z. Wang, "A soft stretchable bending sensor and data glove applications," *Robotics and Biomimetics*, vol. 3, no. 1, p. 22.

[7] J. Wang, C. Lu, and K. Zhang, "Textile-Based Strain Sensor for Human Motion Detection," *Energy & Environmental Materials*, vol. 3, no. 1, pp. 80–100.

[8] K. Chatterjee, J. Tabor, and T. K. Ghosh, "Electrically Conductive Coatings for Fiber-Based E-Textiles," *Fibers*, vol. 7, no. 6, p. 51.

[9] J. Di Tocco, D. Lo Presti, A. Rainer, E. Schena, and C. Massaroni, "Silicone-Textile Composite Resistive Strain Sensors for Human Motion-Related Parameters," *Sensors*, vol. 22, no. 10, p. 3954.

[10] C. Ballester, V. Muñoz, D. Copaci, L. Moreno, and D. Blanco, "Design of a soft sensor based on silver-coated polyamide threads and stress-strain modeling via Gaussian processes," *Sensors and Actuators A: Physical*, vol. 367, p. 115058.

[11] K.-H. Ha, H. Huh, Z. Li, and N. Lu, "Soft Capacitive Pressure Sensors: Trends, Challenges, and Perspectives," *ACS Nano*, vol. 16, no. 3, pp. 3442–3448.

[12] C. Sánchez, D. Rodríguez, S. Otero, and C. A. Monje, "Enhancing sensing performance of 3D-printed TPU/CB piezoresistive strain sensors through integration of silver ink IDE," *Sensors and Actuators A: Physical*, vol. 393, p. 116757.

[13] Shieldex®, "Shieldex®Nice." `https://www.shieldex.com/product/shieldex-nice/`. Accessed: July 22, 2025.

[14] Smooth-On, Inc., "Ecoflex™ 00-35 fast." `https://www.smooth-on.com/products/ecoflex-00-35/`. Accessed: July 22, 2025.

[15] Y.-F. Wang, T. Sekine, Y. Takeda, J. Hong, A. Yoshida, H. Matsui, D. Kumaki, T. Nishikawa, T. Shiba, T. Sunaga, and S. Tokito, "Printed Strain Sensor with High Sensitivity and Wide Working Range Using a Novel Brittle–Stretchable Conductive Network," *ACS Applied Materials & Interfaces*, vol. 12, no. 31, pp. 35282–35290.

[16] Y.-F. Wang, A. Yoshida, Y. Takeda, T. Sekine, D. Kumaki, and S. Tokito, "Printed Directional Bending Sensor with High Sensitivity and Low Hysteresis for Human Motion Detection and Soft Robotic Perception," *Sensors*, vol. 23, no. 11, p. 5041.

[17] L. Nagua, C. Relaño, C. A. Monje, and C. Balaguer, "A New Approach of Soft Joint Based on a Cable-Driven Parallel Mechanism for Robotic Applications," *Mathematics*, vol. 9, no. 13, p. 1468.

[18] C. A. Monje, C. Relaño, L. F. Nagua, S. Martínez, and C. Balaguer, "Eslabón para articulación blanda y articulación blanda que comprende dicho eslabón." Patent reference P202030726. Universidad Carlos III de Madrid, 2024-06-19.